Polymer 50 (2009) 6149–6156

Contents lists available at ScienceDirect

Polymer

journal homepage: www.elsevier.com/locate/polymer

A variable energy positron annihilation lifetime spectroscopy study of physical aging in thin glassy polymer films

Brandon W. Rowe [a], Steven J. Pas [b], Anita J. Hill [b], Ryoichi Suzuki [c], Benny D. Freeman [a], D.R. Paul [a,*]

[a] Department of Chemical Engineering, Texas Materials Institute and Center for Energy and Environmental Resources, The University of Texas at Austin, Austin, Texas 78712, USA
[b] CSIRO Materials Science and Engineering, Private Bag 33, Clayton, Victoria 3168, Australia
[c] National Institute of Advanced Industrial Science and Technology (AIST), Tsukuba, Ibaraki, Japan

ARTICLE INFO

Article history:
Received 14 August 2009
Received in revised form
18 October 2009
Accepted 20 October 2009
Available online 24 October 2009

Keywords:
Free volume
Physical aging
Polymer membranes

ABSTRACT

The influence of physical aging on the profile of free volume characteristics in thin polysulfone (PSF) films was investigated using variable energy positron annihilation lifetime spectroscopy. The PSF films exhibited decreasing *o*-Ps lifetime during physical aging, while *o*-Ps intensity remained constant. The *o*-Ps lifetime was reduced at lower implantation energies, indicating smaller free volume elements near the film surface (i.e., in the top ~50 nm). These near-surface regions of the films age dramatically faster than bulk PSF. The accelerated aging is consistent with the notion of enhanced mobility near the film surface, which allows polymer near the surface to reach a lower free volume state more quickly than the bulk. No influence of the silicon wafer support on aging behavior was detected. Additionally, the impact of CO_2 conditioning on physical aging was briefly examined. The results from these studies were compared to aging behavior of ultrathin PSF films tracked by gas permeability measurements, and favorable agreement was found.

© 2009 Elsevier Ltd. All rights reserved.

1. Introduction

Glassy polymers are inherently non-equilibrium materials that evolve over time towards thermodynamic equilibrium, a process termed physical aging [1]. Physical aging is manifested by changes in the polymer's physical properties over time (e.g., density, refractive index, permeability, etc.) [2–5]. These changes can significantly alter the performance of devices containing glassy polymers, making it essential to study and understand aging behavior. Physical aging of bulk polymers has been studied extensively, and several models have been developed to describe the behavior [2,6–8]. Glassy polymer applications (e.g., microelectronics, separation membranes, optical materials, and lithography), however, often utilize the material in thin film form [9–12]. Initially, it was believed that the aging behavior of thin films would follow that of the bulk material; however, reports have shown that physical aging can be very sensitive to sample dimensions [4,13–18]. For example, in polymers used to create gas separation membranes, the physical aging rate can become orders of magnitude more rapid, as compared to bulk behavior, when the film thickness is reduced below about one micron [4]. This phenomenon has broad implications in several technologies, and an improved understanding of how physical dimensions affect aging rates will allow more accurate predictions of the long-term performance of ultrathin glassy polymer films.

Significant effort has focused on understanding the influence of confinement on the glass transition behavior of ultrathin polymer films (i.e., less than 100 nm thick) [19–23]. Free standing films and films supported on non-attractive substrates are suggested to have a region of enhanced mobility near the film surfaces; this enhanced mobility results in decreased T_g as film thickness is reduced [22,24,25]. Conversely, films supported on attractive substrates have mobility restrictions at the polymer–substrate interface that can cause an increase in T_g with decreasing film thickness [26,27]. These deviations in glass transition behavior can influence physical aging behavior, as shown by Priestley et al. [28]. However, T_g changes are typically not evident at film thicknesses above ~100 nm, while thickness-dependent changes in aging behavior can arise in films that are *microns* thick. It is not fully understood why the changes in physical aging behavior exist at length scales far beyond that expected from studies of the dynamics of ultrathin films. However, deviation from bulk behavior can be larger at lower temperatures, perhaps causing the deviation to manifest itself at larger length scales in these materials far below T_g [29,30].

Studying the mechanisms responsible for accelerated aging in thin polymer films is ongoing, and several models have been

* Corresponding author. Tel.: +1 512 471 5392; fax: +1 512 471 0542.
E-mail address: drp@che.utexas.edu (D.R. Paul).

0032-3861/$ – see front matter © 2009 Elsevier Ltd. All rights reserved.
doi:10.1016/j.polymer.2009.10.045

proposed to describe the behavior, including the diffusion of free volume and thickness-dependent lattice contraction [31–34]. These models can often describe thin film aging data as shown by Huang and Paul, and McCaig et al. [32,33]; yet, if the thickness-dependent factors have no physical significance, they become merely fitting parameters. Verification of these models remains elusive due to the shortage of suitable experimental techniques to test their assumptions. Several techniques, including tracking gas permeability, ellipsometry, and fluorescence spectroscopy, have been used to study physical aging in thin glassy polymer films [4,18,35]. These techniques, however, probe integrated properties of the entire film. Therefore, they cannot provide details regarding the spatial dependence of properties, such as density, across the film and the evolution of the spatial dependence of such properties with aging. To validate the proposed models, the free volume, or density, profile within the film and its time dependence should be characterized.

Positron annihilation lifetime spectroscopy (PALS) is a unique experimental technique capable of determining the size and concentration of free volume sites in amorphous polymers by measuring the lifetime of injected positrons [36]. The lifetime of positrons that annihilate as *ortho*-positronium (*o*-Ps), τ_3, depends on the size of the free volume cavity in which they are located and can, therefore, be related to the size of free volume elements in the sample [36–42]. A spherical cavity shape is traditionally assumed, using the relationship shown in equation (1) to relate τ_3 and cavity size:

$$\tau_3 = \frac{1}{2}\left[1 - \frac{r}{r+\Delta r} + \frac{1}{2\pi}\sin\left(\frac{2\pi r}{r+\Delta r}\right)\right]^{-1} \tag{1}$$

where r is the cavity radius and Δr is the e^- layer thickness (1.656 Å). Additionally, the fraction of positrons that annihilate as *o*-Ps, the *o*-Ps intensity (I_3), is related to the concentration of free volume elements in a polymer.

PALS has been used to study the changes in free volume characteristics during physical aging for a variety of amorphous polymers [43–48]. Depending on the nature of the polymer, these studies report a decrease in the free volume element size (τ_3) and/or concentration (I_3) with physical aging. One of the earliest studies using PALS to track physical aging, by Jean et al., reported decreases in τ_3 with annealing time below T_g in an amine-cured epoxy resin containing diglycidyl ether of bisphenol-A [49]. Conversely, physical aging in polycarbonate resulted in decreased *o*-Ps intensity while τ_3 remained constant, as reported by Hill and Agrawal [44]. The standard PALS technique uses high energy positrons that penetrate deeply (on the order of 100 μm) into amorphous polymers and, therefore, probes the average properties of bulk systems, with no ability to study the influence of surfaces or film thickness on free volume.

The coupling of PALS with a variable mono-energetic positron beam source has resulted in a relatively new technique that allows the energy of the incident positron beam, and, therefore, penetration depth, to be controlled from a few nanometers to several microns [50–53]. The median implantation depth, $z_{1/2}$, and mean implantation depth, z_0, are given in nm by:

$$z_{1/2} = \frac{28.1}{\rho(z)}E^{1.71} \tag{2a}$$

$$z_0(E) = z_{1/2}(E)(\ln 2)^{-1/2} \tag{2b}$$

where ρ is the polymer density in g/cm^3 and E is the incident positron beam energy in keV [54,55]. This ability to selectively control the positron implantation depth enables the free volume to be studied as a function of distance from the surface, allowing the nature of the free volume profile within a polymer film to be characterized. The implantation-stopping profile, $P(z)$, also a function of the beam energy, broadens as the implantation energy increases [54,55]. Equation (3) shows the dependence of $P(z)$ on implantation depth:

$$P(z) = -\frac{\mathrm{d}}{\mathrm{d}z}\left\{\exp\left[-\left(\frac{z}{z_0(E,\rho(z))}\right)\right]^2\right\} \tag{3}$$

There are only a few reports on the use of this technique to study thin polymer films [50,52,56–58]. Polystyrene, the most commonly studied polymer using this technique, was shown by Cao et al. and Algers et al. to have increased *o*-Ps lifetime near the polymer surface [56,57]. Additionally, the *o*-Ps intensity was shown to decrease near the films surface; this result was attributed to a fraction of the positrons diffusing back out of the film and annihilating as free positrons in the vacuum surrounding the sample.

How the free volume profile in a polymer film evolves during physical aging is not currently understood, even though such information is essential for determining the mechanisms behind accelerated aging in thin glassy films. In this work, variable energy PALS was utilized to study the age-dependent profile of free volume characteristics in thin polysulfone films. The utility of this technique to probe physical aging in thin glassy polymer films is demonstrated. The results were analyzed to evaluate the influence of the free surface on physical aging. Additionally, the results were directly compared to aging studies of gas permeability of ultrathin films, and favorable agreement was found.

2. Experimental section

2.1. Materials and film preparation

Bisphenol A-based polysulfone (PSF) from Solvay Advanced Polymers with a glass transition temperature, T_g, of 186 °C was used as received in this study. This polymer was selected based on its utility in the gas separation industry and existing knowledge of its aging behavior. Thin films ($l \sim 450$ nm) were prepared by spin casting a 5 wt% polymer solution of cyclopentanone onto silicon wafers at 1000 rpm for 60 s. A variable angle spectroscopic ellipsometer manufactured by J.A. Woollam Co., model 2000D, was used to measure film thickness. Using de-ionized water, the thin PSF films were lifted from the silicon support onto thin wire frames and heated 15 °C above the bulk T_g in a N_2 purged oven for 20 min to erase any previous history [59]. The films were then rapidly quenched to the aging temperature, defining the start time for the aging studies. The films were subsequently aged, either in a free-standing state on the thin wire frame or supported on a silicon wafer, in a dry environment at 35 °C.

Thick PSF films ($l \sim 100$ μm) were prepared by solution casting from methylene chloride onto silicon wafers using metal casting rings and glass plates to slow evaporation. The films were dried for one week at room temperature, at 100 °C in a vacuum oven for two days, and finally heated to 230 °C for 30 min to remove any residual solvent and remove prior history. The thick films were then rapidly quenched to the aging temperature to define the starting time of the aging studies.

2.2. Positron annihilation lifetime spectroscopy (PALS)

PALS measurements were performed using an automated EG&G Ortec fast–fast coincidence system with BaF scintillators and a resolution of 260 ps (^{60}Co source with the energy windows set to ^{22}Na events). Polymer films were stacked (~1 mm thick) on either

side of a 30 μCi ^{22}NaCl foil (2.54 μm Ti) source, and wrapped in aluminum foil. At least 10^6 counts are collected for each measurement, and each spectrum took approximately 30 min to collect. Data analysis was performed using LT9. The spectra were best fitted with three components with the shortest lifetime fixed to 125 ps, characteristic of *p*-Ps annihilation [36]. Only the *ortho*-positronium (*o*-Ps) components with the longest measured lifetimes, (τ_3), and its intensities, I_3, were considered further since they are ascribed to annihilations in free volume cavities of the polymer matrix [36].

2.3. Variable energy PALS

The variable energy PALS experiments were conducted at the intense slow positron beam facility at the National Institute of Advanced Industrial Science and Technology (AIST) in Tsukuba, Japan [53]. Positron lifetime spectra were collected by measuring the time between the signal from the pulsing system and the annihilation γ-ray detected by a BaF_2 scintillation detector. Spectra were collected for energies from 0.3 keV to 5.4 keV, with at least 10^6 counts at each energy measured. The time resolution of the apparatus was 250–480 ps dependent on incident energy. Experiments were performed under high vacuum at 25 °C. More details on the intense slow positron beam facility have been reported by Suzuki et al. [50,53]. All variable energy PALS experiments were performed using films supported on 15 mm × 20 mm pieces of silicon wafer. Films aged or treated in the free standing state were placed on the silicon support immediately before testing.

3. Results and discussion

3.1. Variable energy PALS measurements

Positron lifetime spectra for 0.3 and 3.0 keV implantation energies in a 450 nm thick PSF film are shown in Fig. 1. These spectra are representative of the data sets collected and analyzed in this work. The data analysis procedure is important because different evaluation methods can result in different estimates of free volume characteristics, as discussed by Algers et al. [56]. Several evaluation methods were considered, including the use of background correction and fitting to three or four lifetimes, with all methods yielding consistent results. The fitting procedure which most accurately fit the data was to remove the energy-dependent background signal from each raw spectrum using reference spectrum from a Kapton film and fit the resulting spectrum to three lifetimes, with the shortest lifetime fixed to 125 ps, characteristic of the *p*-Ps lifetime. This procedure was used to analyze all of the data reported in this study.

3.2. Physical aging of supported PSF films

Fig. 2 presents the *o*-Ps lifetime as function of mean positron implantation depth for 450 nm thick PSF films aged for various times on a silicon wafer support. Each dataset represents a different sample that was aged for the specified time, after quenching from above T_g, at 35 °C in a dry environment prior to measurement. The *o*-Ps lifetime decreases at all implantation depths during the physical aging process, corresponding to a decrease in the average free volume element size with aging, as expected. After aging for ~3000 h, τ_3 decreased by ~0.1 ns across the entire PSF film. Interestingly, relative to the center of the film, τ_3 is reduced near the surface of the PSF films, to a depth of ~50 nm, at all aging times, indicating smaller free volume elements near the film surface. These results contrast with the behavior reported for other polymers studied using this technique, including polystyrene, where τ_3 increases at low implantation energies [50,56–58,60]. Although the aging history of other polymers studied using variable energy PALS is unclear and may contribute to the different depth-dependent behavior of τ_3, this finding indicates some difference in the nature of the near-surface region in these polymers. A recent study by Ata et al. showed polystyrene had similar τ_3 values at penetration depths of 8.8 nm and 350 nm, suggesting that the influence of the free surface extends less than 8.8 nm into the film in the case of polystyrene, which is a significantly smaller region than seen in the PSF studied here [61]. Furthermore, an additional long-lived lifetime component at low implantation energies has been reported and may increase *o*-Ps lifetime estimates if not accounted for by fitting an additional lifetime or removing the Kapton reference background, as was done here [56,62]. The *o*-Ps lifetimes at higher implantation energies in PSF are also lower than in the film center, indicating reduced free volume element size near the back surface of the film. The τ_3 profile is not symmetric with respect to the film center because the range of depth probed, in addition to the average depth, increases with increasing implantation energy, causing reduced depth sensitivity at higher energies [55].

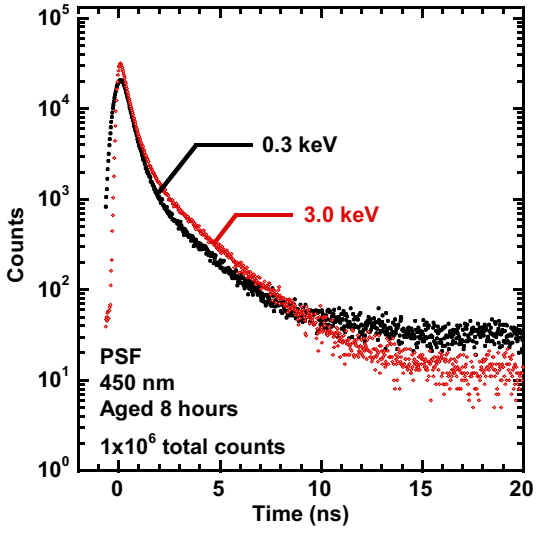

Fig. 1. Positron lifetime spectra of polysulfone film from variable energy positron beam at incident energies of 0.3 keV (●) and 3.0 keV (◇).

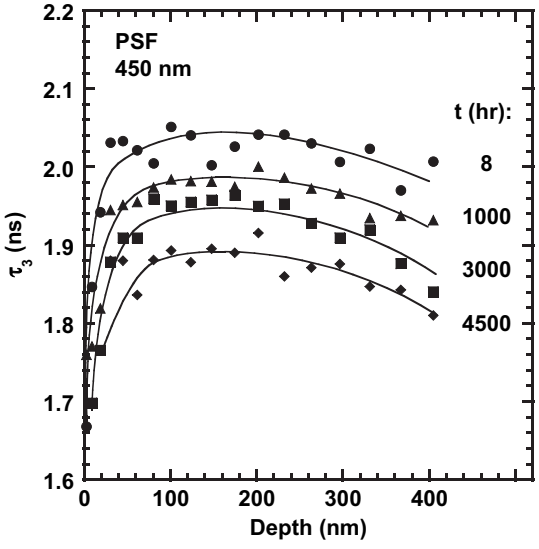

Fig. 2. Influence of positron implantation depth and physical aging on *o*-Ps lifetime in thin PSF films. Lines are provided to guide the eye.

The *o*-Ps intensity data for the PSF films studied are presented in Fig. 3. Physical aging did not have a significant influence on the I_3 profile in the PSF films studied, indicating the number of free volume elements did not change measurably during the aging process. The I_3 decrease near the film surface resulted from the population of positrons that diffused from the near-surface of the film and annihilated in vacuum as free positrons. Conversely, at higher implantation energies, a portion of positrons annihilated in the silicon support instead of in the polymer film and caused the decrease in I_3 at deeper implantation depths.

The influence of physical aging on the profile of free volume characteristics in PSF presented here suggests a thickness-dependent lattice-contraction type mechanism is responsible for accelerated aging in thin glassy films. This accelerated aging is thought to result from enhanced mobility near the film surface that allows it to reach lower free volume more rapidly than the bulk, resulting in smaller free volume elements near the film surface, as seen in Fig. 2. Accelerated aging results are also well described in terms of diffusion based models [32,34]; however, in this case, the number of free volume elements does not change with time as would be expected if diffusion of free volume dominated the aging process.

3.3. Comparison of physical aging in free standing and supported PSF films

Studies have shown property differences between free standing and supported ultrathin films (i.e., $l < 100$ nm), depending on the polymer/substrate interactions present [22,63]. In addition to influences on the glass transition behavior, strong attractive polymer/substrate interactions were thought to cause the suppressed aging in a 20 nm poly(methyl methacrylate) film on a silicon substrate, as compared to a 500 nm film [28]. Although the free-standing case was not studied, this result illustrates the possible influence of substrate interactions on physical aging.

In this work, the PSF films were not strongly bonded to the silicon support, as they were easily separated at any time, and the films were significantly thicker than films shown to have substrate-dependent properties. A previous report, on identical PSF samples, demonstrated a strong correlation between the aging behavior of supported films studied by ellipsometry and free standing films studied by gas permeability measurements, indicating minimal influence of the silicon support on aging [33]. To further investigate the influence of the silicon support on physical aging in PSF films, the free volume characteristics of PSF films aged with and without the silicon wafer support were studied using variable energy PALS. The films aged without the silicon wafer support were supported by thin wire frames, attached on only two sides, allowing the film to age in a free-standing state. Note that due to experimental requirements, films aged in the free standing state were placed on a silicon support immediately before testing. Fig. 4 a and b present the *o*-Ps lifetime and intensity profiles, respectively, for PSF films aged for 8 and 3000 h in both the free standing and supported states. The free volume characteristics are identical, within experimental error, at each aging time for both sets of films, indicating the silicon support had no significant influence on aging in the 450 nm thick PSF films, as might be expected in view of the weak adhesive bond.

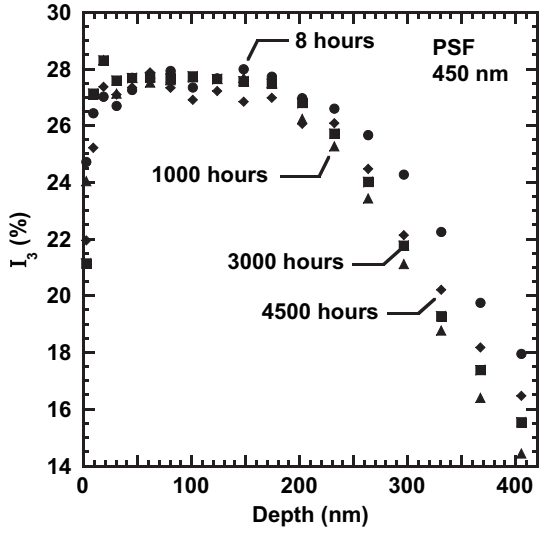

Fig. 3. Influence of positron implantation depth and physical aging on *o*-Ps intensity in thin PSF films.

3.4. Influence of previous history on physical aging

The state of a glassy polymer and, correspondingly, its aging behavior depend not only on its contiguous environment, but also on its previous history (e.g., thermal, stress, vapor exposure) [64,65]. In

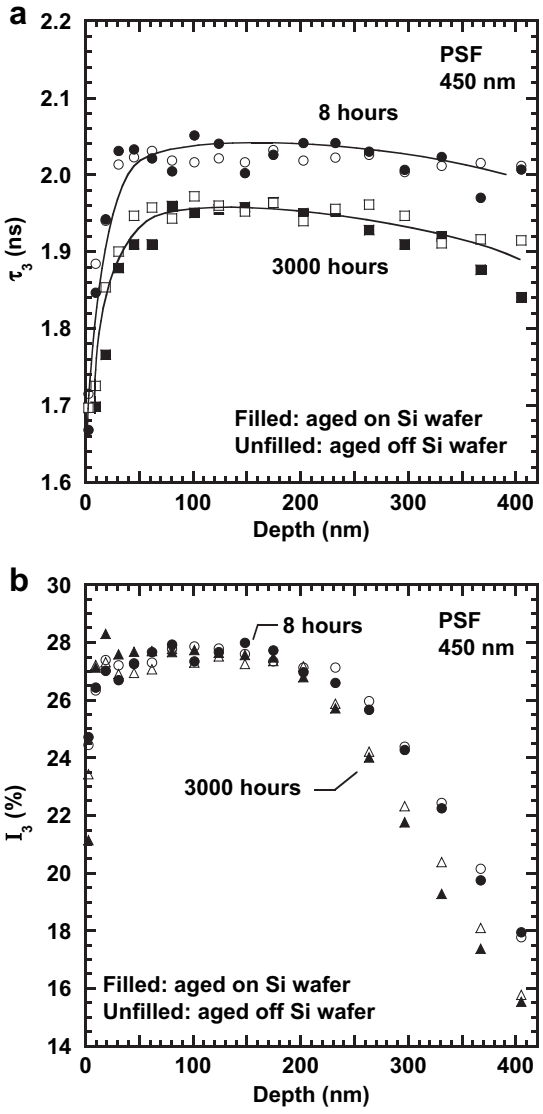

Fig. 4. *o*-Ps Lifetimes (a) and intensities (b) versus mean implantation depth for PSF films aged for 8 and 3000 h supported on a silicon wafer (filled symbols) and in a freestanding state (unfilled symbols). Lines are provided to guide the eye.

addition to thermal treatments, there are a number of ways the free volume state of glassy polymers can be altered. For example, exposure to high pressure CO_2 causes glassy polymers to swell, and upon removal of the CO_2, the system is unable to immediately return to its previous state, leaving the polymer in a lower density state [66–68]. While the effects of this conditioning treatment are not immediately reversible, the polymer may return to its original state by physical aging (i.e., changes due to conditioning are semi-permanent). Application of mechanical stress and exposure to highly sorbing vapors can also induce these types of changes in glassy polymers [69,70]. Glassy polymers used commercially have complex histories arising from their production, storage, and delivery, making it is essential to understand how this previous history affects subsequent aging behavior. However, limited information on this issue exists because only the freshly quenched state is typically studied.

The influence of previous history on the aging behavior of thin PSF films was investigated using variable energy PALS. In the standard case, the PSF film was aged after a rapid quench from above T_g; in the conditioned case, the PSF film was quenched from above T_g, aged for 500 h, and exposed to 800 psig CO_2 for 24 h before the experimental aging time began. Fig. 5 displays the profile

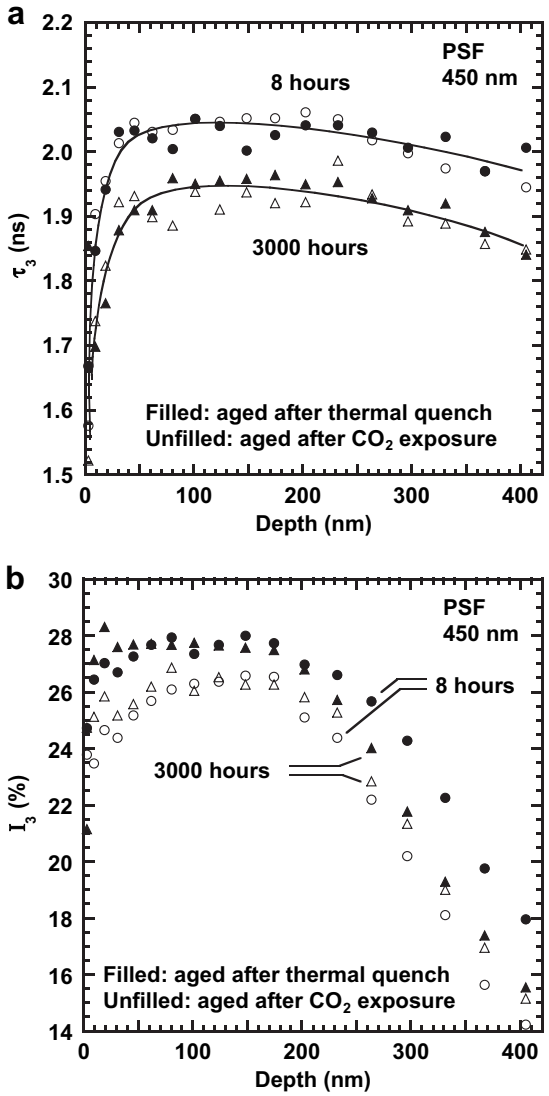

Fig. 5. *o*-Ps Lifetimes (a) and intensities (b) versus mean implantation depth for PSF films aged for 8 and 3000 h after a thermal quench (filled symbols) and after conditioning with CO_2 (unfilled symbols). Lines are provided to guide the eye.

of free volume characteristics of the films aged with these two different histories. The CO_2 conditioning returned the free volume elements to the same size as after the thermal quench from above T_g, indicating the conditioning and thermal quench had similar influences on the free volume element size in PSF, shown in Fig. 5 a. A similar increase of τ_3 in bulk PSF upon exposure to high pressure CO_2 was reported by Yuan et al. [71]. Moreover, the free volume elements in the conditioned films contracted similarly during physical aging as in the thermally quenched case. While the behavior of the τ_3 profile was similar in the two cases studied, the concentration of free volume elements, as related to I_3, was altered significantly. Upon conditioning by CO_2, I_3 decreased throughout the PSF film, indicating a decrease in the number of free volume holes, shown in Fig. 5 b. For instance, at a mean implantation depth of 100 nm, I_3 decreased from 27.5% in the thermally quenched case to 26% in the conditioned case, independent of aging time. This result, in connection with the increase in τ_3 upon conditioning, suggests that free volume elements combined to some extent during the exposure to high pressure CO_2 after aging for 500 h. Consistent with the behavior after a thermal quench, the I_3 profile did not change significantly with aging time in the conditioned films. These findings suggest that although the conditioned films have a different free volume distribution than the thermally quenched samples, physical aging progresses similarly in both cases.

3.5. Comparison with bulk physical aging behavior

Fig. 6 a and b show the aging response of bulk PSF ($l \sim 1$ mm) after a quench from above T_g, tracked using the standard PALS technique. As in the thin film aging studies, the *o*-Ps lifetime decreased with physical aging while I_3 was unchanged. The value of τ_3 measured in the bulk material, 1.96 ns, is similar to that measured in the thin films during this study and to bulk values reported in the literature [71,72]. However, the bulk measurements give slightly lower *o*-Ps intensity values than the thin films studied in this work. Similar deviations between *o*-Ps intensity measured using the standard technique and variable energy beams exist. For instance, Hu et al. reported an I_3 of ~15% for poly(methyl methacrylate) (PMMA) measured using the standard technique, while variable energy PALS studies by Algers et al. show an I_3 of 30% in PMMA [56,73].

A comparison of the aging behavior (i.e., the change in τ_3 with time) between the bulk and thin film state of PSF is shown in Fig. 7. Clearly, physical aging is significantly accelerated in the thin film as compared to the bulk, in agreement with the results from gas permeability studies on PSF [4]. Indeed, the change in τ_3 with aging was ~5 times greater in the thin film than in the bulk samples. This result provides further evidence of the substantial impact that free surfaces have on the physical aging behavior of thin glassy PSF films.

3.6. Impact of the free surface on physical aging

The free volume characteristics measured using variable energy PALS allows the influence of the free surface on physical aging to be examined. The average *o*-Ps lifetime across a specific depth of film, $\bar{\tau}_3$, can be calculated using equation (4):

$$\bar{\tau}_3 = \frac{\sum(\tau_{3i} \times \Delta l_i)}{l} \tag{4}$$

where τ_{3i} is the *o*-Ps lifetime across the distance Δl_i and l is the total film depth analyzed. Fig. 8 presents the average *o*-Ps lifetime as a function of aging time for three regions of the film studied; the

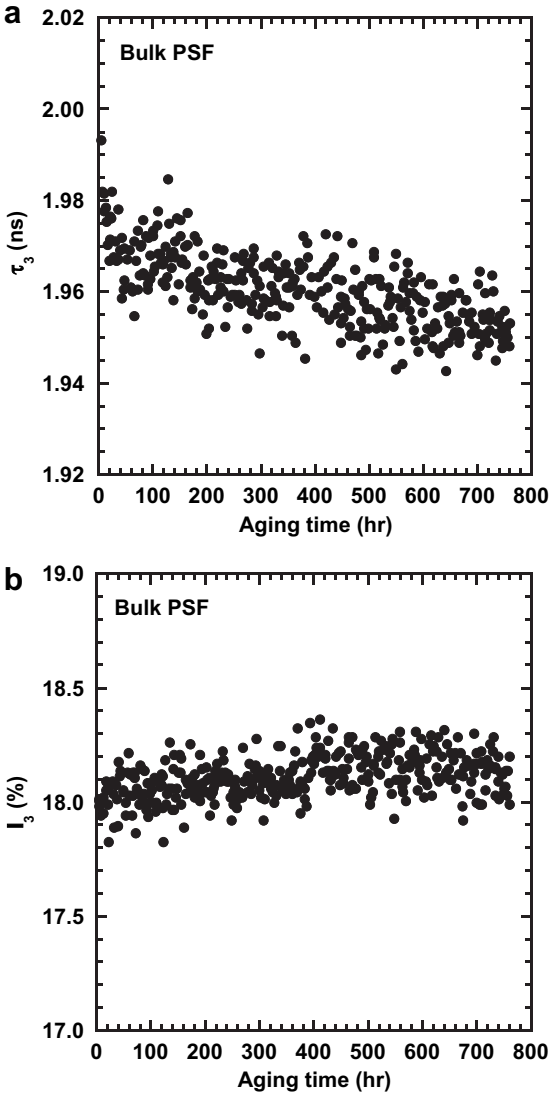

Fig. 6. Influence of aging time on *o*-Ps lifetime (a) and intensity (b) in bulk PSF.

surface to 50 nm deep, the surface to 125 nm deep, and through the entire 450 nm film. The inset in Fig. 8 illustrates the regions of interest. $\bar{\tau}_3$ decreases with physical aging in each case. The decrease in $\bar{\tau}_3$ with physical aging is similar for all penetration depths, ~0.1 ns from 8 to 3000 h of aging, indicating that physical aging progresses in the same way throughout the film during this aging period despite the deviation in free volume properties across the film depth. As the total penetration depth increases, the average *o*-Ps lifetime at each aging time increases, a result from the lower *o*-Ps lifetime in the near-surface region of the films studied. It is believed that the smaller free volume elements near the film surface result from enhanced mobility in the near-surface region over the bulk (i.e., the free volume elements near the surface aged more rapidly, and are therefore smaller, as compared to the bulk after the first eight hours of aging). Standard aging models might suggest that the smaller free volume elements near the surface would age more slowly due to the decreased driving force (i.e., smaller free volume elements might be expected to be closer to equilibrium) as compared to the film center. However, the enhanced mobility of the near-surface region, relative to the bulk, counterbalances the reduced driving force, resulting in a similar decrease of free volume element size with time after 8 h of aging throughout the film.

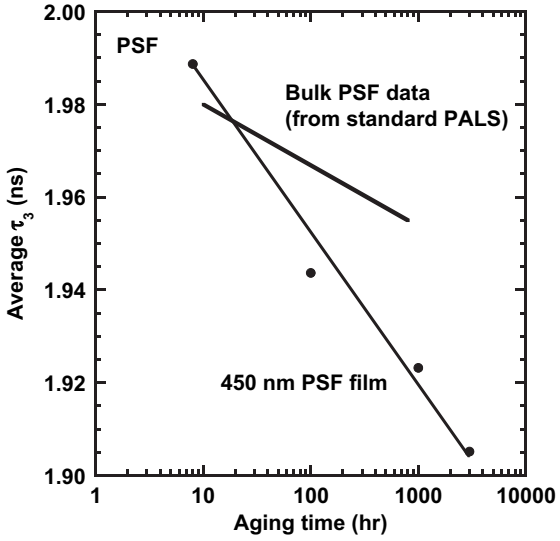

Fig. 7. Comparison of the influence of physical aging on the *o*-Ps lifetime of a 450 nm PSF film and bulk PSF. Line provided to guide the eye.

3.7. Comparison with gas separation studies

Tracking gas permeability properties is another method used to study the influence of film thickness and the free surface on physical aging. To compare the results from the variable energy PALS studies presented here with results from gas permeability studies on ultrathin PSF films, the PALS parameters are first converted to fractional free volume, FFV, or *f*. Correlations in the literature show good agreement between free volume estimates from PALS parameters and from equations of state [36,39,43,74]. The relationship between PALS parameters and free volume can be written as

$$\mathrm{FFV} = C \times I_3 \times v_f(\bar{\tau}_3) \tag{5}$$

where *C* is a constant relating *o*-Ps intensity to the total number of free volume elements and v_f is the average free volume element size, as related to $\bar{\tau}_3$ [36]. While this correlation includes the *o*-Ps

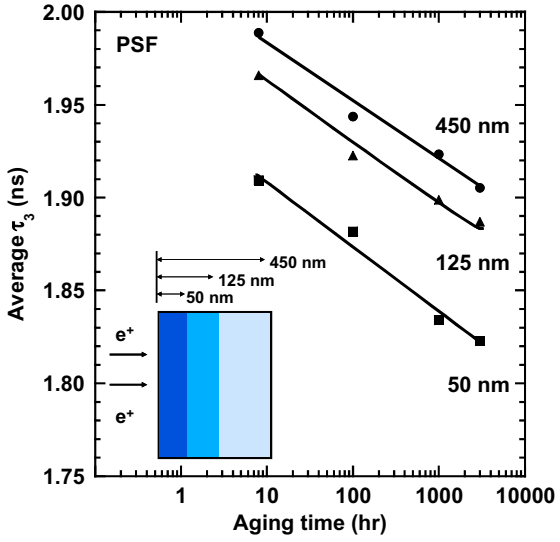

Fig. 8. Influence of physical aging on the *o*-Ps lifetime averaged across several penetration depths of a 450 nm thick PSF film. Inset schematic shows the film regions of interest. Lines are provided to guide the eye.

Table 1
Model parameters.

Parameter	Value
FFV	0.1560
τ_3 (ns)	1.96
C' (ns^{-3})	0.0206
A (Barrer)	397
B	0.839

1 Barrer $= 1 \times 10^{-10}$ [cm^3(STP) cm/(cm^2 sec cmHg)].

intensity, this factor was not considered here because no aging dependence on I_3 was detected, and the influence of the surface and silicon substrate on I_3 is an artifact of the experimental technique that is not well characterized. Equation (6) shows the connection between FFV and $\bar{\tau}_3$ used in this work:

$$\mathrm{FFV} = C' \times \bar{\tau}_3^3 \tag{6}$$

where C' is a constant related to the number of free volume elements. Here, C' can be calculated using the FFV calculated from bulk density and group contribution theory [75], and $\bar{\tau}_3$ from PALS measurements on bulk PSF using the standard technique. Since r and $\bar{\tau}_3$ are proportional across the range considered here, $\bar{\tau}_3^3$ is used in place of $^4/_3\Pi r^3$ to represent the free volume element size. Furthermore, Maurer and Schmidt showed equation (6) more accurately follows the free volume data from PVT measurements and the Simha–Somcynsky equation-of-state theory than equation (5), at least in the case of PMMA [39]. Then, gas permeability, P, can be calculated using the following correlation:

$$P = A \times e^{-B/\mathrm{FFV}} \tag{7}$$

where A and B are constants from literature correlations based on bulk polymers [76]. The parameters used in this equation are shown in Table 1. Finally, equations (6) and (7) can be combined to provide the following connection, which contains no adjustable parameters, between PALS parameters and gas permeability:

$$P = A \times e^{-B/(C' \times \bar{\tau}_3^3)} \tag{8}$$

The data presented in Fig. 8 were used to calculate permeability values as a function of penetration depth and aging time using equation (8); the results are shown in Fig. 9. The gas permeability data in Fig. 9, previously published, were collected on free standing PSF films [77]. There is good agreement between the gas permeability behavior determined by these two very different experimental techniques, especially considering the PALS estimate of permeability was obtained with no adjustable parameters. Both the measured gas permeability data and the permeability estimated from the PALS studies decrease with aging time, as expected. Additionally the initial gas permeability decreases with film thickness; it is suggested that this decrease results from the enhanced mobility of the ultrathin films, which allow them to reach a low free volume state, and therefore a lower permeability, in the time required to prepare the samples for measurement following the quench from above T_g. The similarity in the aging response determined by these two techniques shows the clear connection between changes in free volume due to physical aging and gas permeability.

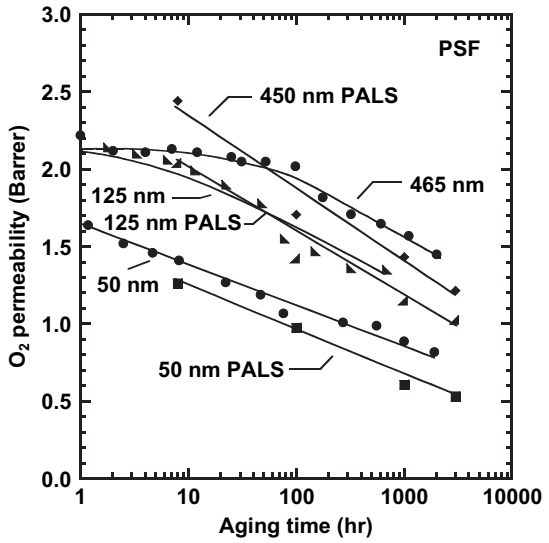

Fig. 9. Comparison of O_2 permeability estimated from o-Ps lifetime data during physical aging of a 450 nm thick PSF film with O_2 permeability measured directly from PSF films of different thickness. Lines are provided to guide the eye. 1 Barrer $= 1 \times 10^{-10}$ [cm^3(STP) cm/(cm^2 sec cmHg)].

4. Conclusions

The influence of physical aging on the profile of free volume characteristics in thin PSF films was studied using variable energy PALS. The loss of free volume accompanying physical aging-induced densification was manifested by the shrinking of free volume elements. As expected, the aging behavior of these PSF films was not noticeably influenced by the presence of a silicon wafer support. While the influence of aging on o-Ps lifetime, related to the free volume element size, was similar between CO_2 conditioned and thermally quenched films, the o-Ps intensity was lower in the CO_2 conditioned films. The influence of the free surface on physical aging was examined and aging was shown to progress similarly across the entire depth of the PSF film. Gas permeability values were calculated directly from the variable energy PALS results and compared with measured permeability data. Excellent agreement between these two experimental techniques illustrates the connection between changes in free volume and gas permeability properties caused by physical aging. Enhanced mobility near the film surface, which allows the region to achieve a lower free volume state more quickly than the bulk, is believed to cause the reduction in free volume size measured near the PSF film surface and contribute to the accelerated aging in thin films as compared to the bulk.

Acknowledgements

This research was supported by Air Liquide/MEDAL, the National Science Foundation (Grant DMR 238979 administered by the Division of Material Research – Polymer Program), the NSF Science and Technology Center for Layered Polymeric Systems (Grant DMR-0423914), an ARC Australian Postdoctoral Fellowship (SJP), and the ARC Australian Centre of Excellence in Electromaterials Science.

References

[1] Struik LCE. Physical aging in amorphous polymers and other materials. Amsterdam: Elsevier; 1978.
[2] Hodge IM. Science 1995;267(5206):1945–7.
[3] Hutchinson JM. Progress in Polymer Science 1995;20(4):703–60.
[4] Huang Y, Paul DR. Polymer 2004;45(25):8377–93.
[5] Kim JH, Koros WJ, Paul DR. Polymer 2006;47(9):3104–11.
[6] Tool AQ. Journal of Research of the National Bureau of Standards 1945;34:199–211.
[7] Kovacs AJ, Aklonis JJ, Hutchinson JM, Ramos AR. Journal of Polymer Science Polymer Physics Edition 1979;17(7):1097–162.
[8] Diezemann G. Journal of Non-Crystalline Solids 2006;352(42–49):4934–40.
[9] Ulbricht M. Polymer 2006;47(7):2217–62.
[10] Bita I, Yang JKW, Jung YS, Ross CA, Thomas EL, Berggren KK. Science 2008;321(5891):939–43.

[11] Ruiz R, Kang H, Detcheverry FA, Dobisz E, Kercher DS, Albrecht TR, et al. Science 2008;321(5891):936–9.
[12] Ibn-Elhaj M, Schadt M. Nature 2001;410(6830):796–9.
[13] Pfromm PH, Koros WJ. Polymeric Materials Science and Engineering 1994;71:401–2.
[14] Dorkenoo KD, Pfromm PH. Macromolecules 2000;33(10):3747–51.
[15] McCaig MS, Paul DR. Polymer 2000;41(2):629–37.
[16] Kim JH, Koros WJ, Paul DR. Polymer 2006;47(9):3094–103.
[17] Huang Y, Paul DR. Macromolecules 2006;39(4):1554–9.
[18] Ellison CJ, Kim SD, Hall DB, Torkelson JM. The European Physical Journal E Soft Matter 2002;V8(2):155–66.
[19] Jackson CL, McKenna GB. Journal of Non-Crystalline Solids 1991;131–133(Part 1):221–4.
[20] Keddie JL, Jones RAL, Cory RA. EPL (Europhysics Letters) 1994;27(1):59–64.
[21] Kim JH, Jang J, Zin WC. Langmuir 2000;16(9):4064–7.
[22] Forrest JA, Dalnoki-Veress K. Advances in Colloid and Interface Science 2001;94(1–3):167–95.
[23] Forrest JA, Dalnoki-Veress K, Stevens JR, Dutcher JR. Physical Review Letters 1996;77(10):2002.
[24] Ellison CJ, Torkelson JM. Nature Materials 2003;2(10):695–700.
[25] Mundra MK, Ellison CJ, Behling RE, Torkelson JM. Polymer 2006;47(22): 7747–59.
[26] Roth CB, McNerny KL, Jager WF, Torkelson JM. Macromolecules 2007;40(7):2568–74.
[27] Labahn D, Mix R, Schonhals A. Physical Review E (Statistical, Nonlinear, and Soft Matter Physics) 2009;79(1):011801–9.
[28] Priestley RD, Broadbelt LJ, Torkelson JM. Macromolecules 2005;38(3):654–7.
[29] Napolitano S, Lupascu V, Wubbenhorst M. Macromolecules 2008;41(4): 1061–3.
[30] Baschnagel J, Binder K. Macromolecules 1995;28(20):6808–18.
[31] Curro JG, Lagasse RR, Simha R. Macromolecules 1982;15(6):1621–6.
[32] McCaig MS, Paul DR, Barlow JW. Polymer 2000;41(2):639–48.
[33] Huang Y, Wang X, Paul DR. Journal of Membrane Science 2006;277(1–2): 219–29.
[34] Cangialosi D, Wubbenhorst M, Groenewold J, Mendes E, Schut H, van Veen A, et al. Physical Review B Condensed Matter and Materials Physics 2004;70(22):2242131–224213111.
[35] Kawana S, Jones RAL. European Physical Journal E Soft Matter 2003;10(3):223–30.
[36] Mallon PE. Application to polymers. In: Jean YC, Mallon PE, Schrader DM, editors. Positron & positronium chemistry. New Jersey: World Scientific; 2003. p. 253–80.
[37] Dlubek G, Kilburn D, Bondarenko V, Pionteck J, Krause-Rehberg R, Alam MA. Macromolecular Symposia 2004;210(Reactive Polymers 2003):11–20.
[38] Yampolskii YP. Russian Chemical Reviews 2007;76(1):59–78.
[39] Maurer FHJ, Schmidt M. Radiation Physics and Chemistry 2000;58(5–6): 509–12.
[40] Tao SJ. The Journal of Chemical Physics 1972;56(11):5499–510.
[41] Liu J, Deng Q, Jean YC. Macromolecules 1993;26(26):7149–55.
[42] Eldrup M, Lightbody D, Sherwood JN. Chemical Physics 1981;63(1–2):51–8.
[43] Kobayashi Y, Zheng W, Meyer EF, McGervey JD, Jamieson AM, Simha R. Macromolecules 1989;22(5):2302–6.
[44] Hill AJ, Heater KJ, Agrawal CM. Journal of Polymer Science Part B Polymer Physics 1990;28(3):387–405.
[45] Davis WJ, Pethrick RA. European Polymer Journal 1998;34(12):1747–54.
[46] Nagai K, Freeman BD, Hill AJ. Journal of Polymer Science Part B Polymer Physics 2000;38(9):1222–39.
[47] Cangialosi D, Schut H, van Veen A, Picken SJ. Macromolecules 2003;36(1): 142–7.
[48] Staiger CL, Pas SJ, Hill AJ, Cornelius CJ. Chemistry of Materials 2008;20(8):2606–8.
[49] Jean YC, Sandreczki TC, Ames DP. Polymeric Materials Science and Engineering 1985;53:185–90.
[50] Jean YC, Cao H, Dai GH, Suzuki R, Ohdaira T, Kobayashi Y, et al. Applied Surface Science 1997;116:251–5.
[51] Dlubek G, Börner F, Buchhold R, Sahre K, Krause-Rehberg R, Eichhorn KJ. Journal of Polymer Science Part B Polymer Physics 2000;38(23):3062–9.
[52] Jean YC, Zhang J, Chen H, Li Y, Liu G. Spectrochimica Acta Part A Molecular and Biomolecular Spectroscopy 2005;61A(7):1683–91.
[53] Suzuki R, Kobayashi Y, Mikado T, Ohgaki H, Chiwaki M, Yamazaki T, et al. Japanese Journal of Applied Physics Part 2 Letters 1991;30(3B):L532–4.
[54] Schultz PJ, Lynn KG. Reviews of Modern Physics 1988;60(3):701.
[55] Algers J, Sperr P, Egger W, Kögel G, Maurer FHJ. Physical Review B 2003;67(12):125404.
[56] Algers J, Suzuki R, Ohdaira T, Maurer FHJ. Polymer 2004;45(13):4533–9.
[57] Cao H, Yuan JP, Zhang R, Sundar CS, Jean YC, Suzuki R, et al. Applied Surface Science 1999;149(1–4):116–24.
[58] Algers J, Suzuki R, Ohdaira T, Maurer FHJ. Macromolecules 2004;37(11): 4201–10.
[59] Huang Y, Paul DR. Journal of Membrane Science 2004;244(1–2):167–78.
[60] Jean YC, Mallon PE, Zhang R, Chen H, Wu YC, Li Y, et al. Applications of slow positrons to polymeric surfaces and coatings. In: Jean YC, Mallon PE, Schrader DM, editors. Positron & positronium chemistry. New Jersey: World Scientific; 2003.
[61] Ata S, Muramatsu M, Takeda J, Ohdaira T, Suzuki R, Ito K, et al. Polymer 2009;50(14):3343–6.
[62] Xie L, DeMaggio GB, Frieze WE, DeVries J, Gidley DW, Hristov HA, et al. Physical Review Letters 1995;74(24):4947.
[63] Priestley RD, Mundra MK, Barnett NJ, Broadbelt LJ, Torkelson JM. Australian Journal of Chemistry 2007;60(10):765–71.
[64] Berens AR, Hodge IM. Macromolecules 1982;15(3):756–61.
[65] Hodge IM, Berens AR. Macromolecules 1982;15(3):762–70.
[66] Chan AH, Paul DR. Journal of Applied Polymer Science 1979;24(6): 1539–50.
[67] Wonders AG, Paul DR. Journal of Membrane Science 1979;5:63–75.
[68] Fleming GK, Koros WJ. Macromolecules 1986;19(8):2285–91.
[69] Enscore DJ, Hopfenberg HB, Stannett VT, Berens AR. Polymer 1977;18(11):1105–10.
[70] Berens AR, Hodge IM. Polymer Engineering and Science 1984;24(14):1123–9.
[71] Yuan J-P, Cao H, Hellmuth EW, Jean YC. Journal of Polymer Science Part B Polymer Physics 1998;36(17):3049–56.
[72] Malhotra BD, Pethrick RA. European Polymer Journal 1983;19(6):457–9.
[73] Hu C-C, Fu Y-J, Hsiao S-W, Lee K-R, Lai J-Y. Journal of Membrane Science 2007;303(1––2):29–36.
[74] Kilburn D, Dlubek G, Pionteck J, Alam MA. Polymer 2006;47(22):7774–85.
[75] Krevelen DWV. Properties of polymers. 3rd ed. Amsterdam: Elsevier; 1990.
[76] Park JY, Paul DR. Journal of Membrane Science 1997;125(1):23–39.
[77] Rowe BW, Freeman BD, Paul DR. Polymer 2009;50(23):5565–75.